Presynaptic Evidence for Zinc Release at the Mossy Fiber Synapse of Rat Hippocampus

Joshua K. Ketterman and Yang V. Li[*]

Department of Biomedical Science, Neuroscience Program, Ohio University, Athens, Ohio

Vesicular zinc (Zn^{2+}) is found in a subset of glutamatergic nerve terminals throughout the mammalian forebrain and is colocalized with glutamate. Despite well-documented neuromodulatory roles, exocytosis of endogenous Zn^{2+} from presynaptic terminals has never been directly demonstrated, because existing studies have measured elevated Zn^{2+} concentrations by examining the perfusate. Thus, the specific origin of synaptic Zn^{2+} remains a controversial subject. Here, we describe synaptic Zn^{2+} trafficking between cellular compartments at hippocampal mossy fiber synapses by using the fluorescent indicator Zinpyr-1 to label the hippocampal mossy fiber boutons. We determined endogenous Zn^{2+} exocytosis by direct observation of vesicular Zn^{2+} as decreasing fluorescence intensity from presynaptic axonal boutons in the stratum lucidum of CA3 during neural activities induced by the stimulation of membrane depolarization. This presynaptic fluorescence gradually returned to a level near baseline after the withdrawal of moderate stimulation, indicating an endogenous mechanism to replenish vesicular Zn^{2+}. The exocytosis of the synaptic Zn^{2+} was also dependent on extracellular Ca^{2+} and was sensitive to Zn^{2+}-specific chelators. Vesicular Zn^{2+} loading was sensitive to the vacuolar-type H^+-ATPase inhibitor concanamycin A, and our experiments indicated that blockade of vesicular reloading with concanamycin A led to a depletion of that synaptic Zn^{2+}. Furthermore, synaptic Zn^{2+} translocated to the postsynaptic cell body upon release to produce increases in the concentration of weakly bound Zn^{2+} within the postsynaptic cytosol, demonstrating a feature unique to ionic substances released during neurotransmission. Our data provide important evidence for Zn^{2+} as a substance that undergoes release in a manner similar to common neurotransmitters. © 2007 Wiley-Liss, Inc.

Key words: synaptic transmission; neurotransmission; neuromodulator; neurotransmitter; fluorescence imaging

The synaptic Zn^{2+} is densely concentrated in the presynaptic vesicles of certain glutamatergic nerve terminals in areas throughout the mammalian forebrain, including the cortex and limbic regions, with particularly high concentrations in the hippocampal mossy fiber pathway (Haug, 1967; Perez-Clausell and Danscher, 1985). This Zn^{2+} is stainable by a variety of histological procedures and has been shown to be weakly bound and freely reactive, thus earning it the name "chelatable" or "free" zinc. The anatomical location of this cation and its possible colocalization with glutamate have led to the hypothesis that vesicular Zn^{2+} is released from presynaptic boutons during synaptic transmission and functions as a neuromodulator. This hypothesis has been supported by evidence from studies employing electrophysiology, fluorescence imaging, microdialysis, and radioligand binding assay (Assaf and Chung, 1984; Howell et al., 1984; Perez-Clausell and Danscher, 1986; Aniksztejn et al., 1987; Vogt et al., 2000; Li et al., 2001b; Ueno et al., 2002; Qian and Noebels, 2005).

An enormous body of research suggests diverse actions of Zn^{2+} on synaptic transmission. N-methyl-D-aspartate (NMDA) receptor-mediated responses are inhibited by zinc in both a voltage-dependent and a voltage-independent manner (Peters et al., 1987; Westbrook and Mayer, 1987). Synaptically released Zn^{2+} may thus play an important role in shaping NMDA receptor responses at mossy fiber-CA3 synapses (Vogt et al., 2000) and in proper in vivo functioning of glycinergic neurotransmission (Hirzel et al., 2006). Zinc also attenuates GABA receptor-mediated responses (Westbrook and Mayer, 1987; Smart et al., 1994; Buhl et al., 1996; Fisher and Macdonald, 1998) and potentiates AMPA receptor-mediated responses (Rassendren et al., 1990). Zinc chelation has also been shown to arrest long-term potentiation (LTP) in the mossy fiber→CA3 circuit of the hippocampus (Li et al., 2001a) and in corticoamygdala synapses (Kodirov et al., 2006).

Zn^{2+} may be the first metal ion ever suggested as a substance that undergoes release like a neurotransmitter during synaptic transmission (Frederickson et al., 2005). However, there has been no direct evidence of exocytosis

or depletion of vesicular Zn^{2+} during neurotransmission. To establish the release of vesicular Zn^{2+} during synaptic transmission, it is imperative to demonstrate that the released Zn^{2+} originated from the presynaptic nerve terminals or boutons. In previous experiments, synaptically released Zn^{2+} has been indirectly studied by measuring elevated Zn^{2+} concentrations in the perfusate (Assaf and Chung, 1984; Howell et al., 1984). More recent fluorescent imaging studies of Zn^{2+} release during neural activities focused on the extracellular space or the postsynaptic cell body (Li et al., 2001b; Ueno et al., 2002; Qian and Noebels, 2005). Despite current advances in Zn^{2+} neurobiology, no model to directly study the exocytosis of vesicular Zn^{2+} sequestered in presynaptic terminals has yet been described. This is due partially to the notoriously difficult nature of presynaptic studies in situ, where efforts are hampered by the diminutive size of the nerve terminals compared with the conspicuous postsynaptic cell bodies regularly examined with electrophysiology and fluorescent imaging.

It is known that free zinc is essentially absent in the intracellular and extracellular fluid, the estimated concentration ($\sim$1 pM) being below the detection limits for most analytical methods (Frederickson and Bush, 2001). To date, Zn^{2+}-containing presynaptic vesicles are the only known source of such free or chelatable Zn^{2+} in the brain, indicating the requirement of vesicular Zn^{2+} release to initiate any potential Zn^{2+} signals during normal neuronal function. Taking advantage of this unique distribution of chelatable Zn^{2+}, we have visually differentiated the mossy fiber boutons from their postsynaptic counterparts by applying the fluorescent Zn^{2+} indicator Zinpyr-1 in acute hippocampal slices. Zinpyr-1 has a high affinity for Zn^{2+} ($\sim$1 nM) with relative high k_{off} value ($2.3 \times 10^{-3} \ sec^{-1}$), which is appreciated in real-time imaging to study the mobilization of vesicular Zn^{2+}; Zinpyr-1 is membrane permeable and can be passively loaded into cells, properties that allow it to stain the synaptic Zn^{2+} contained within synaptic vesicles (Burdette et al., 2001; Woodroofe et al., 2004; Goldsmith and Lippard, 2006). In our experimental model, we have specifically labeled the Zn^{2+}-containing mossy fiber boutons of the hippocampus while demonstrating a lack of Zinpyr-1 fluorescence in the CA3 pyramidal neurons. Our comprehensive results support the role of vesicular Zn^{2+} as an ion that undergoes release in a manner similar to common neurotransmitters and indicate the possibility of Zn^{2+} as an example of a new class of neuromodulators in the form of divalent transmission metal cations.

MATERIALS AND METHODS

Fluorophores and Chemicals

Zinpyr-1 salts were purchased from NeuroBioTex, Inc. (Galveston, TX). Ethylenediamine tetraacetic acid disodium-calcium salt (CaEDTA), concanamycin A (folimycin), and gadolinium were purchased from Sigma-Aldrich (St. Louis, MO). Unless otherwise noted, all other chemicals and salts were purchased from Sigma-Aldrich Fluka (St. Louis, MO) or Fisher Biotech (Pittsburgh, PA).

Hippocampal Slice Preparation

All experiments were conducted according to the principles outlined in the Ohio University guidelines for the care and handling of animals. Adult male Sprague Dawley rats (200–300 g) were euthanized with CO_2 and decapitated. The brain was quickly removed and incubated for 1 min in 1–4°C artificial cerebrospinal fluid for extraction (sACSF) with the following composition (in mM): NaCl 121, KCl 1.75, $NaHCO_3$ 26, dextrose 10, KH_2PO_4 1.25, $MgCl_2$ 5.0. After incubation, the brain tissue was mounted onto a stage for slicing, and transverse slices of 250 μm were prepared using a Vibratome 3000 zero-Z Plus Automated (The Vibratome Co., St. Louis, MO). Extracted slices were transferred to an incubation chamber containing room-temperature, standard ACSF with the following composition (in mM): NaCl 121, KCl 1.75, $NaHCO_3$ 26, dextrose 10, KH_2PO_4 1.25, $MgCl_2$ 1.3, $CaCl_2$ 2.4. All slices were incubated for 10 min prior to beginning dye protocols and constantly perfused with 95% O_2/5% CO_2 throughout all experiments. The osmolality of all solutions measured in the range of 290–300 mOsm, and the pH was maintained within the physiological range ($\sim$7.4).

Dye Incubation and Zn^{2+} Imaging

One millimolar stock solutions of Zinpyr-1 were prepared and then diluted in ACSF to reach a final concentration of 20 μM. Prepared hippocampal slices were incubated in a 20 μM Zinpyr-1 ACSF solution at room temperature for $\sim$5 min. After dye loading, slices were transferred to a chamber containing standard ACSF and incubated for at least 30 min prior to experimental protocols to wash out excess dye fully and allow the Zn^{2+} signal to reach a stable baseline. Prepared slices were then transferred to an imaging stage and secured in place using an inert nylon mesh stretched over a ring of platinum wire. Solutions were continuously bubbled with 95% O_2/5% CO_2 and perfused onto the imaging stage at a rate of 2 ml/min with a peristaltic pump. Confocal images were taken with a Zeiss inverted confocal microscope (Carl Zeiss, Oberkochen, Germany) and analyzed in Image Pro 5.1 (MediaCybernetics, Silver Spring, MD).

Selection of Regions of Interest and Fluorescence Measurements

To measure mean optic density, series images were observed at time 0. Postsynaptic cell bodies were selected based on focal clarity and an asymmetrical, triangular shape characteristic of a healthy pyramidal cell. Regions of interest (ROI) were drawn as an ellipse over the interior of the postsynaptic cell body using the analysis tools in Image Pro. This ellipse was then copied and placed over an area of presynaptic fluorescence in the stratum lucidum of the CA3 region of the hippocampus. The area of presynaptic fluorescence was chosen based on spatial proximity (<50 μm from the original ROI) and uniform fluorescence that provided a stark contrast to the postsynaptic cell body (see Figs. 1, 2). After selection of

ROIs, mean optic density was determined by using the Track Objects tool in Image Pro, and optical data were copied to Microsoft Excel 2003 for statistical analysis.

The initial fluorescence F_0 was determined by averaging the baseline fluorescence over 10 min before treatment. For endogenous Zn^{2+} experiments with line scans, F_0 was determined by averaging the last 100 fluorescence readings prior to termination of high-frequency stimulation (ΔF in line scan experiments was determined by averaging the 100 recordings collected at the peak fluorescence change). Data presented in bar charts are thus unitless expressions normalized to the baseline fluorescence recorded for each experiment calculated per the following equation: $\Delta F/F_0 = (F - F_0)/F_0$.

Statistical Analyses

All parametric statistics were conducted in SPSS 14 (SPSS Inc., Chicago, IL) and included t-tests for paired data and one-way ANOVA. Unplanned comparisons of significant differences in ANOVA were performed with Student-Newman-Keuls post hoc tests. Tests for homogeneity of variance were conducted using an F-max test in Microsoft Excel 2005 and Levene's test conducted in SPSS.

RESULTS

Using the Zinpyr-1 fluorophore and the unique distribution of vesicular Zn^{2+}, we developed a presynaptic model to determine the exocytosis of endogenous Zn^{2+} at the MF-CA3 synapse in the mammalian hippocampus. The Zinpyr-1 signal was specific for intracellular Zn^{2+}, and there was little signal in the presence of extracellular Zn^{2+}. Hippocampal slices dyed with Zinpyr-1 revealed compact Zn^{2+} staining along the mossy fiber projections (boutons) at the hilar and CA3 regions of the hippocampus consistent with Timm's stain, the traditional method for detecting intracellular Zn^{2+} (Fig.

1A,B). Zinpyr-1 fluorescence was clearly localized to the stratum lucidum of the CA3 region, where mossy fiber projections from the dentate granule neurons terminate proximal to the basal dendrites of the CA3 pyramidal cells in the stratum pyramidale of the hippocampus (Fig. 1A–C). Closer examination of Zinpyr-1-stained slices allowed us to make a clear visual distinction between areas of bright, presynaptic fluorescence in the stratum lucidum synonymous with Zn^{2+}-containing mossy fiber boutons and dark areas of postsynaptic fluorescence in the form of pyramidal cell bodies of the stratum pyramidale lacking weakly bound, freely reactive Zn^{2+} (Fig. 1D). Examination of the degree of fluorescence among these two regions showed them to be significantly different (Fig. 1E). The strong Zn^{2+} fluorescence from the presynaptic stratum lucidum as well as the low background fluorescence from the stratum pyramidale remained stable for periods >50 min, providing ample time to investigate Zn^{2+} kinetics with pharmacological and electrophysiological techniques. This clear visual distinction between pre- and postsynaptic areas of fluorescence intensity in the mossy fiber→CA3 (MF→CA3) circuit formed the basis of a presynaptic model for studying vesicular Zn^{2+} release and uptake at mossy fiber boutons.

Presynaptic Release of Zn^{2+} From Mossy Fiber Boutons

Synaptic Release of Zn^{2+} Induced by Membrane Depolarization. Depolarization of the neuronal membrane serves as the signal that triggers the release of neurotransmitter from nerve terminals. If Zn^{2+} is released from the presynaptic boutons in a manner similar to common neurotransmitters, its release should be evoked by depolarization of the mossy fiber axons. In

---

Fig. 1. Zinc release as detected by Zinpyr-1. **A:** Hippocampal slice prepared using the Danscher method of Timm's stain (Danscher, 1981), the traditional method for detecting intracellular Zn^{2+}. Note the dark staining pattern in the hilar region of the dentate gyrus (H) as well as the dark zinc-containing mossy fibers in the stratum lucidum of CA3 (C3). **B:** Hippocampal slice loaded with the fluorescent Zn^{2+}-indicator Zinpyr-1 (20 μM). The overall staining pattern for slices with Zinpyr-1 is very similar to that seen in Timm's staining, with bright green areas of fluorescence in the hilar region (H) and the stratum lucidum of CA3 (C3); CA1 (C1) shows far less staining. **C:** With low-magnification (at ×10) microscopy, distinct regions of hippocampal anatomy are clearly visible in slices stained with Zinpyr-1. The mossy fibers containing histochemically active zinc fluoresce brightly in the stratum lucidum (SL) of the CA3 region. The granule cell bodies of the dentate gyrus (DG) show only a low level of background fluorescence similar to the pyramidal cells (PYR, arrows) of the CA3 region (C3). **D:** With a higher magnification (at ×25), pyramidal cell bodies (PYR, arrows) become clearly visible. Zn^{2+}-containing mossy fiber terminals in the SL fluoresce brightly, with individual bright dots of the SL showing a diameter of ∼5 μm, a total area roughly equal to the size of a single synaptic bouton. These small areas of bright fluorescence in comparison with the low level of background fluorescence observed in the stratum pyramidale form the basis of a visual distinction between pre- and postsynaptic regions of interest. **E:** Bar figure showing the degree of fluorescence in the SL (pre, pink bar) and the stratum pyramidale (post, blue bar) of CA3 region of the hippocampus. The fluorescence was normalized to the baseline fluorescence (F_0) of the stratum radiatum in CA1, and the two were significantly different (pre mean = 0.71 ± 0.055, post mean = -0.35 ± 0.054, n = 14, ★$P < 0.001$). **F:** Short exposure (1 min) of slices to 60 mM exogenous K^+ causes a decrease in presynaptic fluorescence that recovers following K^+ washout. This decrease in presynaptic fluorescence is coupled with a simultaneous, transient increase in the fluorescence of the postsynaptic cell body. **G:** Consecutive short exposures (3 min) of Zinpyr-1-stained slices to 60 mM exogenous K^+ followed by washout (5 min) show repeating decrease and recovery of presynaptic fluorescence coupled with steady increases in fluorescence recorded at the postsynaptic cell body. **H:** Quantification of data seen in D. Fluorescence changes seen with the second depolarization event are approximately one-half the magnitude of the initial fluorescence change (1st presynaptic mean = -0.051 ± 0.016, first postsynaptic mean = 0.063 ± 0.017, 2nd presynaptic mean = -0.025 ± 0.008, second postsynaptic mean = 0.03 ± 0.013, n = 4, ★$P < 0.05$).
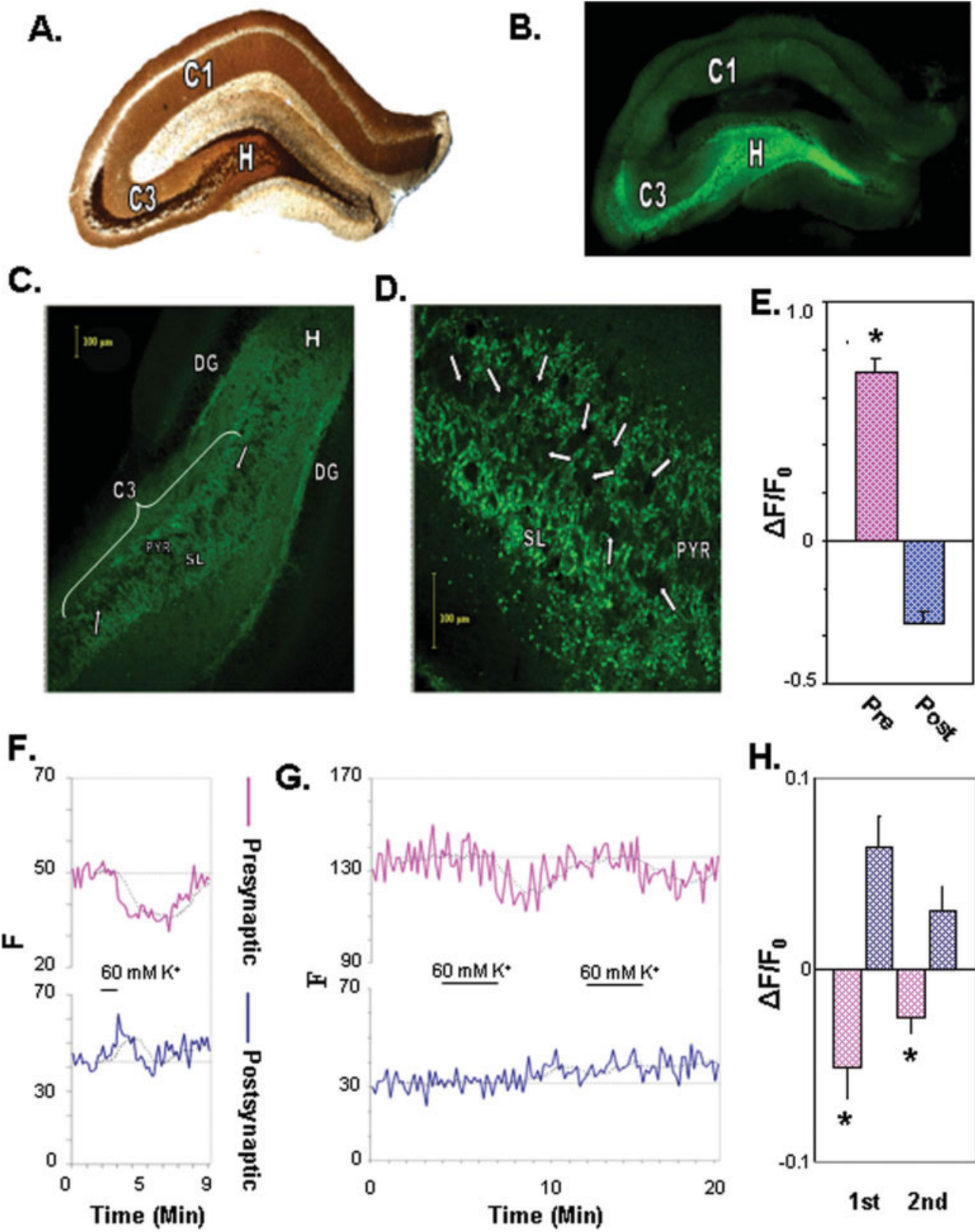
Figure 1.

the current study, depolarization of the neuronal membrane by bath application of exogenous K^+ (60 mM) caused a significant decrease in Zinpyr-1 fluorescence recorded from the mossy fiber boutons. Potassium-enriched ACSF for K^+ depolarization was prepared by substituting K^+ for Na^+ in standard ACSF on a 1:1 basis maintaining the same osmolarity and pH (see Materials and Methods). To observe the synaptic release of endogenous Zn^{2+}, we briefly perfused the hippocampal slices with 60 mM K^+ for 1 min. This treatment induced a decrease in presynaptic fluorescence recorded from the mossy fiber boutons of CA3 (Fig. 1F), indicating the exocytosis of vesicular Zn^{2+} in response to physiologically relevant depolarizing stimulus. After the washout with regular ACSF, presynaptic fluorescence gradually returned to a level near baseline. Exposure to moderate, 3-min, consecutive perfusions of K^+ (60 mM) caused a similar decrease in presynaptic fluorescence (Fig. 1G). Washout of depolarizing media followed by a second treatment with K^+ demonstrated a return to baseline fluorescence during washout, followed by a second decrease in fluorescence when slices were again depolarized (Fig. 1G). Brief application of K^+ thus induced repeated episodes of Zn^{2+} release. The magnitude of fluorescence change during this second depolarizing event was smaller than the first (Fig. 1H; n = 12, $P < 0.001$), indicating that the vesicular pool of Zn^{2+} is susceptible to depletion over time and offering the possibility that the characteristics of Zn^{2+} transmission are susceptible to change due to prior neuronal activities.

To expand on our findings and to characterize unequivocally the exocytosis of vesicular Zn^{2+} at the MF–CA3 synapse, we then examined Zinpyr-1 fluorescence changes during prolonged depolarizing activity. Untreated, the Zinpyr-1 signal remained stable over periods >50 min (Fig. 2A), affording us ample opportunity to explore our model using various pharmacological agents. Bath application of exogenous K^+ (60 mM, 10 min) caused a robust decrease in presynaptic fluorescence coupled with an immediate increase in postsynaptic fluorescence (Fig. 2B). To examine endogenous Zn^{2+} kinetics further, we decreased the level of free vesicular Zn^{2+} by incubating slices in CaEDTA (Fig. 2C), an extracellular chelator of Zn^{2+} ($K_d = 4 \cdot 10^{-16}$ M) known to deplete vesicular Zn^{2+} over time (Frederickson et al., 2002). By incubating slices in CaEDTA (5 mM for 10 min) prior to beginning fluorescence recordings, we expected to decrease vesicular Zn^{2+} and reduce the degree of fluorescence change recorded during perfusion of depolarizing concentrations of exogenous K^+. Preincubated slices showed an overall reduced level of fluorescence, indicating the successful reduction of intracellular Zn^{2+} by CaEDTA. The addition of K^+ (60 mM) to slices preincubated with CaEDTA showed significantly less decrease in the level of Zinpyr-1 fluorescence (or Zn^{2+} exocytosis) recorded from the mossy fiber boutons compared with the untreated group (Fig. 2D, untreated group in Fig. 2B). Together these results further support the idea that depolarization of the neuro-

nal membrane evoked the release or exocytosis of vesicular Zn^{2+} from the mossy fiber boutons.

Blocking Ca^{2+} Influx Prevents Synaptic Release of Zn^{2+} from Mossy Fiber Boutons.   The release of neurotransmitter from nerve terminals is dependent on the influx of extracellular Ca^{2+} through voltage-dependent Ca^{2+} channels. If Zn^{2+} is released in a matter similar to commonly identified neurotransmitters, we would expect its release during neuronal depolarization events to require the influx of exogenous Ca^{2+}. In our model, Ca^{2+}-free perfusion medium (no added Ca^{2+}) prevented the fluorescence reduction in presynaptic mossy fibers in response to K^+-induced depolarization of the neuronal membrane (Fig. 3A), indicating that the release of Zn^{2+} from presynaptic terminals requires the presence of extracellular Ca^{2+}. Blockade of voltage-gated Ca^{2+} channels by gadolinium (5 μM), a voltage-dependent Ca^{2+} channel blocker, produced a similar result (Fig. 3B), indicating the release of vesicular Zn^{2+} is dependent on Ca^{2+} influx through voltage-dependent Ca^{2+} channels. These findings indicate that Zn^{2+} is stored in presynaptic vesicles that are released by an exocytotic process dependent on the influx of Ca^{2+} through voltage-gated calcium channels following depolarization of the neuronal membrane.

Translocation of Synaptically Released Zn^{2+} into Postsynaptic Neuron Following Membrane Depolarization.   Recorded decreases in presynaptic fluorescence were coupled with immediate increases in postsynaptic pyramidal cell body fluorescence (Figs. 1G, 2B, lower traces). The relative degree of change was almost equal and opposite in magnitude for the two synaptic regions (Figs. 1H, 2B′, bar chart; n = 11, $P < 0.01$). This finding revealed a feature unique to vesicular Zn^{2+}: upon release from the presynaptic vesicles, free Zn^{2+} is capable of subsequent translocation to the postsynaptic cell body, producing increases in Zn^{2+} levels within the postsynaptic cytosol (Li et al., 2001b). To examine further the translocation of synaptically released Zn^{2+}, we closely examined the changes of fluorescence in postsynaptic pyramidal neurons. By selecting ROIs that were proximal and distal from the presynaptic ROI, we were able to quantify spatially dependent fluctuations in Zn^{2+} fluorescence. In areas of the postsynaptic cell body proximal to the stratum lucidum, significant increases in fluorescence were noted during depolarizing events (Fig. 4A). Areas close to the center (nucleus) of the postsynaptic cell body actually showed no change or a small decrease in fluorescence (Fig. 4A). This decrease likely was due to reduced fluorescence from Zn^{2+}-releasing mossy fibers outside of the focal plane during confocal microscopy. Quantification of these data revealed that the fluorescence change was comparable to and opposite in magnitude for presynaptic and proximal postsynaptic areas, whereas distal areas in the postsynaptic area showed less fluorescence change (Fig. 4B; n = 4, $P < 0.005$).

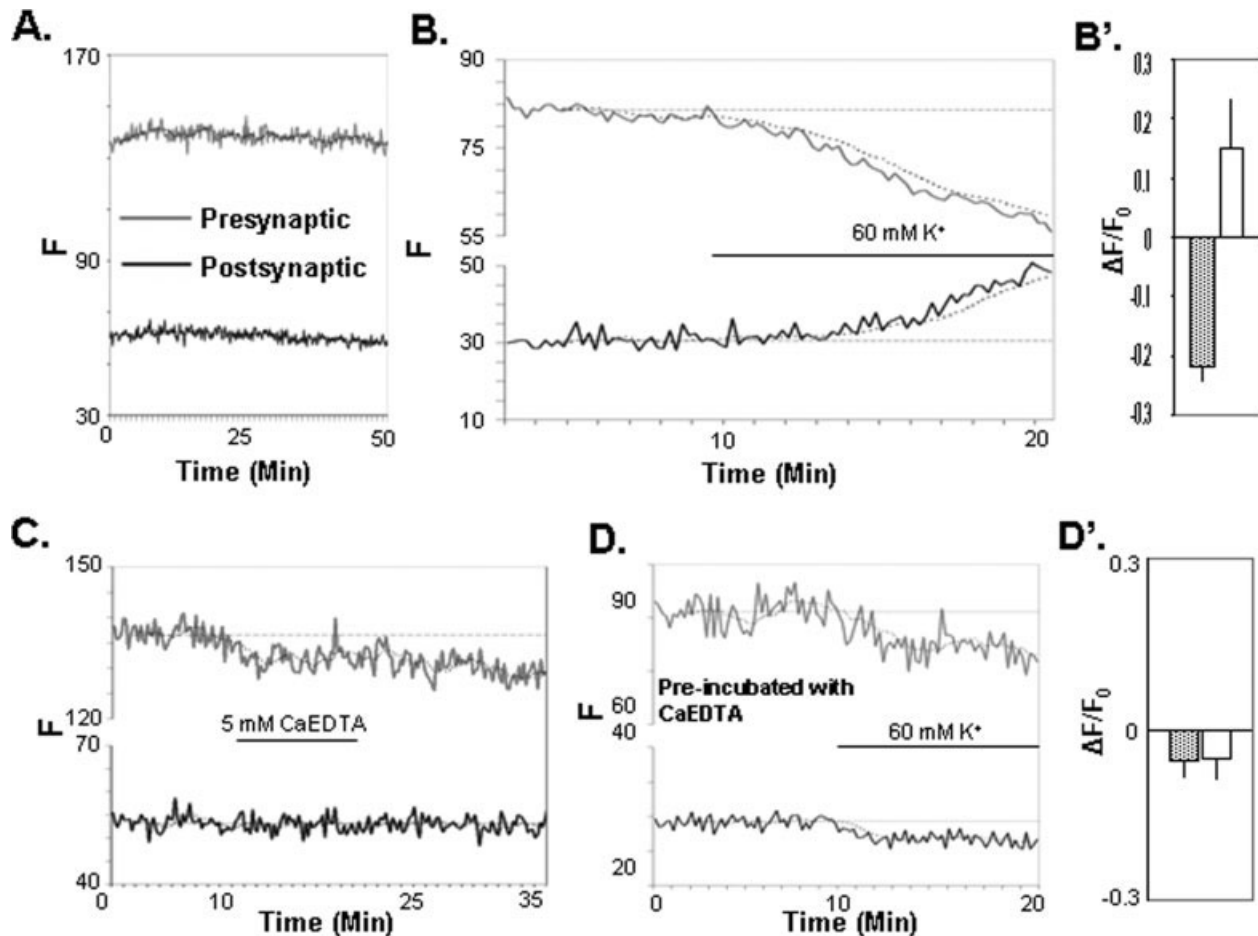To determine that postsynaptic fluorescence increases were due to the translocation of synaptically

Fig. 2. Characteristics of Zn^{2+} release. **A:** Untreated, Zinpyr-1 fluorescence remains steady for periods of ~50 min. **B:** Treatment with 60 mM K^+ for slices stained with Zinpyr-1. Depolarizing concentrations of exogenous K^+ resulted in a decrease in presynaptic fluorescence coupled with a simultaneous increase in postsynaptic fluorescence. **B′:** Bar graph of $\Delta F/F_0$ data for depolarizing K^+ stimulus: differences between pre- and postsynaptic areas were significant [presynaptic mean = -0.22 ± 0.02 (hatched bar), postsynaptic mean = 0.15 ± 0.08 (open bar), n = 11, $P < 0.01$]. **C:** Treatment with the membrane-impermeable Zn^{2+} chelator CaEDTA (5 mM) caused

a reduction in presynaptic fluorescence, indicating the depletion of vesicular Zn^{2+} from the presynaptic mossy fiber terminals by the chelator. **D:** Prechelation of vesicular Zn^{2+} with 5 mM exogenous CaEDTA for 10 min prior to K^+ depolarization was sufficient to deplete vesicular stores of Zn^{2+}, resulting in less fluorescence change when slices were exposed to depolarizing concentrations of exogenous K^+. **D′:** Pre- and postsynaptic regions of interest showed no significant difference in fluorescence change [presynaptic mean = -0.06 ± 0.03 (hatched bar), postsynaptic mean = -0.05 ± 0.03 (open bar), results summarized in bar figure below traces].

released Zn^{2+} and not from contaminating Zn^{2+} present in the perfusion medium, we decided to repeat our depolarizing experiment in the presence of a low concentration CaEDTA (100 μM). Although CaEDTA is a high-affinity Zn^{2+} chelator, this compound has relatively slow kinetics (Martell and Smith, 1974; Davis et al., 1999; Li et al., 2001a). We reasoned that, by employing a lower concentration of CaEDTA, we could remove exogenous Zn^{2+} from the perfusate without compromising the postsynaptic fluorescence signal observed during depolarization of hippocampal slices. Depolarization of slices with 60 mM K^+ in the presence of 100 μM CaEDTA showed a result similar to the control condition, with large decreases in presynaptic fluorescence coupled with postsynaptic fluorescence increases (Fig.

4C). These results support the conclusion that postsynaptic fluorescence increases are due to the translocation of endogenously released Zn^{2+} rather than influx of contaminating Zn^{2+} from the perfusate. However, slices treated with 5 mM CaEDTA in addition to 60 mM exogenous K^+ showed a significant decrease in the presynaptic fluorescent signal but no immediate increase in fluorescence in the postsynaptic region (Fig. 4D). These results indicated that the addition of 5 mM CaEDTA was sufficient to overcome the relatively slow kinetics of CaEDTA chelation and bind Zn^{2+} dynamically as it was released during mossy fiber depolarization, preventing Zn^{2+} translocation to the postsynaptic cell body.

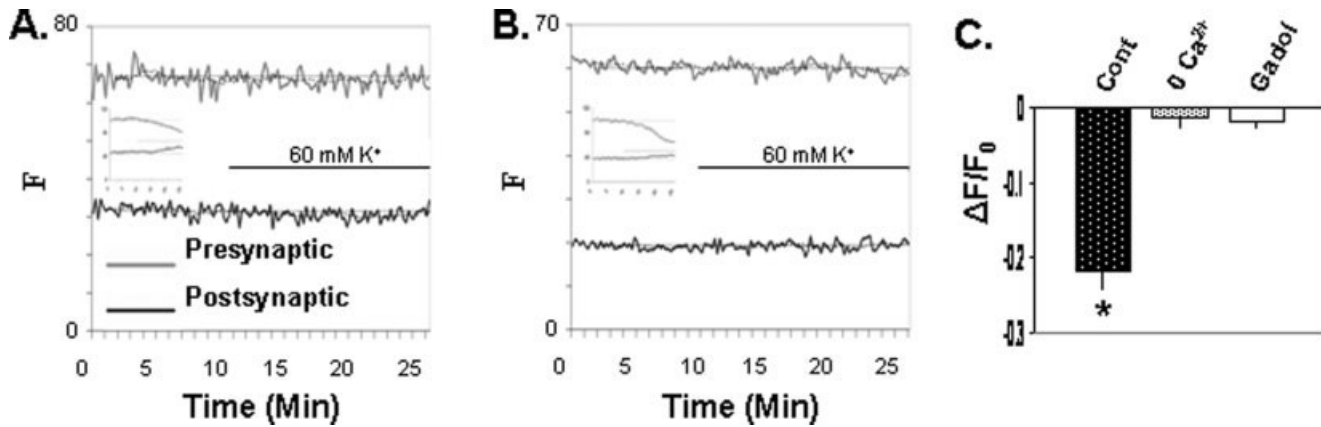**Effects of Concanamycin A (Folimycin).** To examine the colocalization of Zn^{2+} and glutamate, we

Fig. 3. Calcium dependence of Zn^{2+} release. **A:** In Ca^{2+}-free medium, treatment with 60 mM exogenous K^+ caused no appreciable chance in presynaptic or postsynaptic fluorescence, indicating that the release of Zn^{2+} from presynaptic terminals requires exogenous Ca^{2+}. **Inset:** Control experiment in which Zinpyr-1-stained slices were exposed to 60 mM exogenous K^+ in normal (calcium added) medium. **B:** Slices treated with the voltage-dependent Ca^{2+} channel blocker gadolinium (5 μM) showed no appreciable change in pre- or postsynaptic fluorescence when exposed to 60 mM exogenous K^+, indicating the requirement of Ca^{2+} influx through voltage-dependent Ca^{2+} channels as necessary for the release of vesicular Zn^{2+}. **Inset:** Control experiment in which slices were exposed to 60 mM exogenous K^+ in the absence of gadolinium. **C:** Bar graph comparing presynaptic fluorescence changes resulting from depolarizing K^+ stimulus from Ca-free media (no added calcium in ACSF) and gadolinium (Gadol) experiments to control experiments without pharmacological treatments. Fluorescence decreased significantly in the control group in which normal Zn^{2+} release was permitted to occur [control mean $= -0.22 \pm 0.023$ (dark hatched bar), Ca^{2+}-free mean $= -0.014 \pm 0.014$ (light hatched bar), gadolinium-treated mean $= -0.02 \pm 0.007$ (open bar), n = 9, $\star P < 0.001$).

employed concanamycin A (folimycin), a specific inhibitor of the vacuolar-type H^+-ATPase (Bowman et al., 1988; Huss et al., 2002; Mothet et al., 2005). By destroying the electrochemical proton gradient across the vacuolar membrane necessary for the loading of synaptic vesicles, concanamycin A depletes glutamate by preventing the reloading of glutamate that undergoes spontaneous release, a process that has been shown to deplete glutamate significantly from the ready-releasable pool in a matter of seconds. In this study, treatment with 1 μM concanamycin A caused a steady decrease in presynaptic fluorescence similar to that observed with the application of exogenous K^+ (Fig. 5A), indicating a depletion of the ready-release pool of Zn^{2+} in a manner similar to glutamate. To observe the overall effects of concanamycin A on the activity of the CA3 synapse, we applied 60 mM exogenous K^+ after 10 min of treatment with 1 μM concanamycin A (Fig. 5B). The lack of significant fluorescence changes following K^+ treatment supported the conclusion that concanamycin A fully depleted releasable vesicular Zn^{2+} over time by preventing the reloading of synaptic Zn^{2+}.

Synaptic Uptake of Zn^{2+} at Mossy Fiber Boutons

We hypothesized that, if Zn^{2+} undergoes release in a way similar to a neurotransmitter, some mechanism must exist to replenish vesicular Zn^{2+} in the presynaptic boutons. One likely mechanism is the uptake of Zn^{2+} released during synaptic transmission. The actions of such a mechanism should be observable with the application of exogenous Zn^{2+} to our model. We tested this hypothesis by observing the effects of 100 μM exogenous Zn^{2+} treatment on slices stained with Zinpyr-1. Treatment with 100 μM Zn^{2+} induced a gradual increase in presynaptic fluorescence (Fig. 6A). To facilitate the uptake of exogenous Zn^{2+} into the presynaptic boutons of the hippocampal mossy fibers, in some experiments we first reduced vesicular Zn^{2+} by treating the slices with 5 mM CaEDTA (10 min), a treatment that might also increase the number of unbound fluorophores available in the presynaptic boutons and enhance the sensitivity of the model to the uptake of exogenous Zn^{2+}. Washout of CaEDTA and subsequent treatment with 100 μM Zn^{2+} caused a significant increase in fluorescence (Fig. 6B) compared with fluorescence induced with exogenous Zn^{2+} alone (Fig. 6C; n = 7, $P < 0.001$). Taken together, these results support the idea that some mechanism exists for the uptake of synaptically released Zn^{2+} during transmission.

We then tested the reuptake of synaptically released endogenous Zn^{2+}. Anticipating that reuptake would be a fast synaptic event, we employed confocal line scans of the mossy fiber connections in the stratum lucidum of the CA3 region to achieve a high degree of temporal resolution. Synaptic Zn^{2+} release was achieved by depolarizing mossy fiber boutons with short, high-frequency electrical stimulation (HFS; 100 Hz, 10 sec). Membrane depolarization by HFS evoked a decrease in fluorescence at the mossy fiber boutons in a manner similar to depolarization by exogenous K^+ (Fig. 6D). This decrease in presynaptic fluorescence intensity likely was due to the rapid release of Zn^{2+} from the mossy fiber terminals.
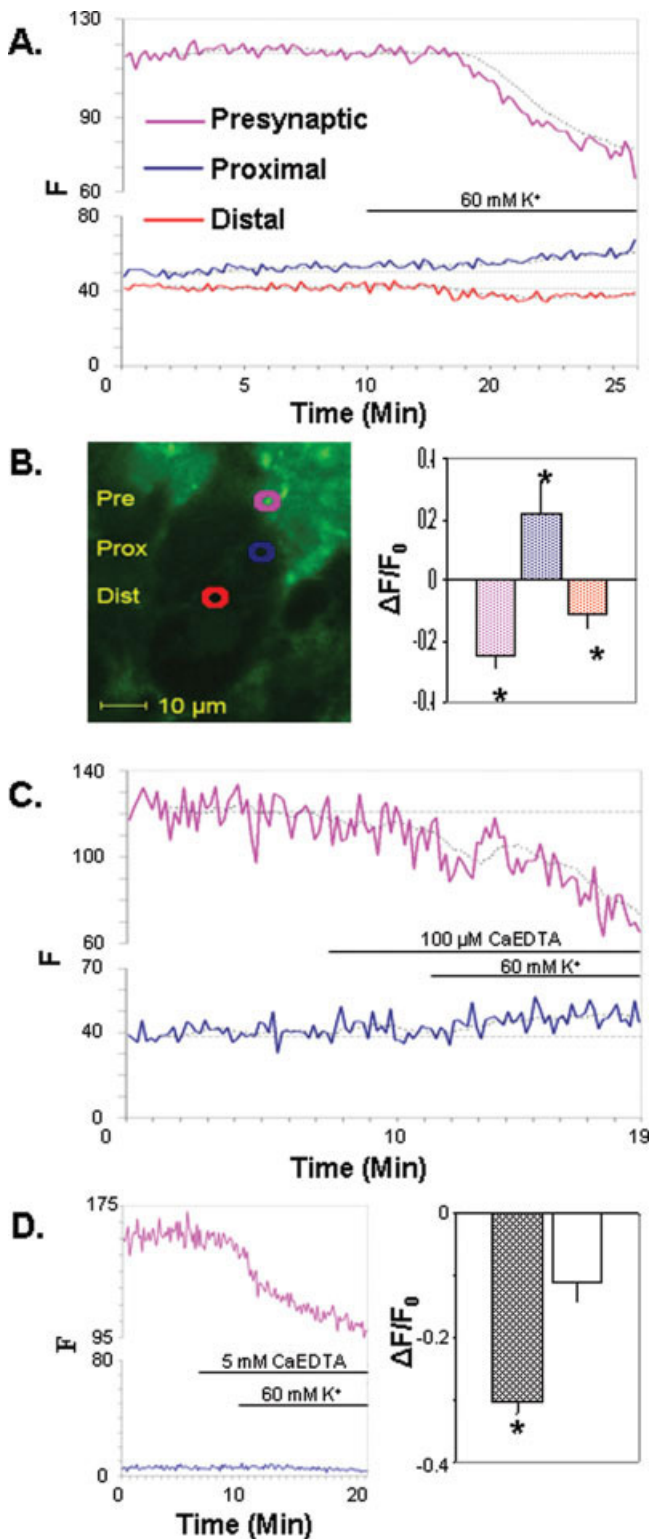
Immediately after withdrawal of the test stimulus, a significant increase or a "hump" in fluorescence was noted in the presynaptic area of the MF→CA3 circuit (Fig. 6D), a phenomenon we attributed to the reuptake of endogenous, synaptically released Zn^{2+}. The increase in fluorescence lasted for several seconds before fluorescence regression, which likely was due to diffusion of the $[Zn^{2+}]_i$ transient. If this fluorescence increase was caused by the reuptake of endogenous Zn^{2+}, we would expect the cell-impermeable, extracellular Zn^{2+}-specific chelator CaEDTA to block reuptake by dynamically chelating Zn^{2+} as it is released into the synaptic cleft. To test this hypothesis, we repeated HFS in the presence of 5 mM exogenous CaEDTA. In the CaEDTA-treated group, the fluorescence transient (hump) was not observed (Fig. 6E). Comparing the mean fluorescence change after electrical stimulation over seven trials, we found that the fluorescence change or the hump in untreated slices was significantly greater than that observed in the presence of CaEDTA (Fig. 6F; n = 7, $P < 0.001$). Taken together, these data suggest the existence of an active mechanism of reuptake to replenish synaptically released Zn^{2+} into the vesicles of the mossy fiber boutons and possibly arrest potential Zn^{2+} signals because of the release of free Zn^{2+} during synaptic transmission.

Fig. 4. Zn^{2+} translocation. **A:** The degree of postsynaptic fluorescence observed was dependent on the spatial location of the region of interest. Fluorescence decreased in the presynaptic ROI with treatment by 60 mM exogenous K^+ (pink line). In ROIs selected from within the postsynaptic ROI very close to the pyramidal cell membrane next to the stratum lucidum, fluorescence increases were at their highest (blue line). ROIs selected from deep within the pyramidal cell body showed a slight decrease in fluorescence (orange line) likely resulting from decreasing background noise from loss of fluorescence from mossy fibers outside of the focal plane. **B:** Left image shows the spatial location and size (~5 μm, roughly the size of a single presynaptic bouton) of presynaptic, proximal, and distal ROIs. Bar graph at right compares fluorescence changes in different spatial locations within the postsynaptic body. A one-way analysis of variance revealed these means to be significantly different [presynaptic mean = −0.25 ± 0.043 (blue bar), proximal mean = 0.22 ± 0.10 (pink bar), distal mean = −0.11 ± 0.046 (orange bar), n = 4, ★$P < 0.005$]. **C:** Fluorescence increases in response to depolarizing stimuli were still visible in the postsynaptic regions presence of 100 μM CaEDTA, indicating that the fluorescence increases in the postsynaptic regions were due to endogenous translocation of synaptic Zn^{2+} as opposed to influx of contaminating Zn^{2+} from the perfusate. **D:** Treatment with 60 mM exogenous K^+ in the presence of 5 mM CaEDTA. Depolarizing K^+ concentrations resulted in a decrease in fluorescence in the presynaptic area but no simultaneous increase in postsynaptic fluorescence, indicating the dynamic binding of synaptically released Zn^{2+} to CaEDTA as effective in blocking Zn^{2+} translocation [presynaptic mean = −0.303 ± 0.02 (hatched bar), postsynaptic mean = −0.111 ± 0.029 (open bar), n = 9, ★$P < 0.025$; results summarized in bar figure below traces].
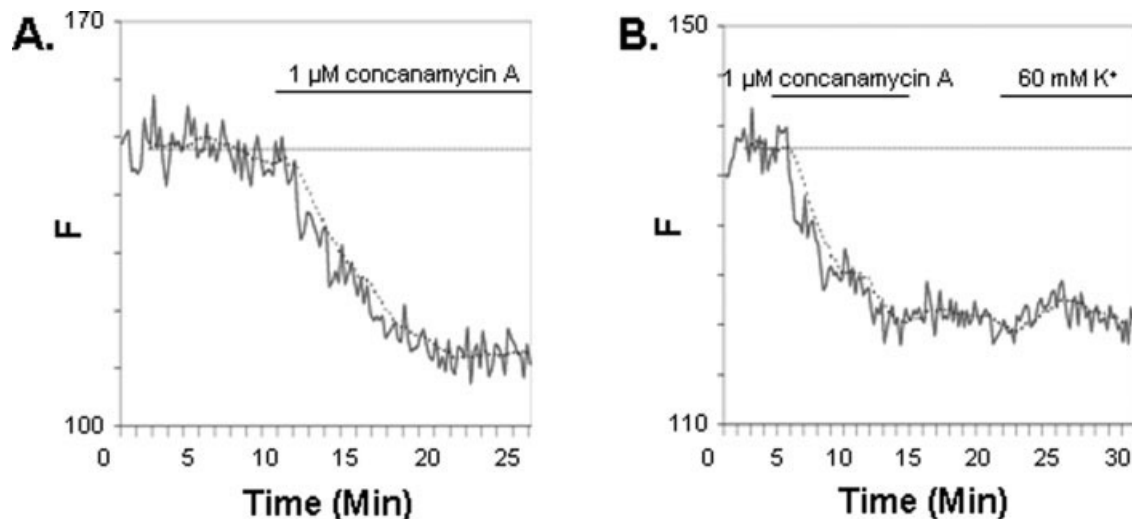
Fig. 5. Zn^{2+} activity depends on the vacuolar-type H^+-ATPase. **A:** Treatment with 1 µM concanamycin A causes a decrease in fluorescence, because spontaneously released Zn^{2+} can no longer be reloaded into the synaptic vesicles (mean change = −0.37 ± 0.03, n = 12). Note that this change is due to the spontaneous release of Zn^{2+} as opposed to release induced by depolarization. **B:** Application of 60 mM exogenous K^+ following treatment with 1 µM concanamycin A caused no significant change in fluorescence, indicating that concanamycin A treatment was sufficient to reduce Zn^{2+} activity in the MF-CA3 synapse in a manner similar to glutamate.

DISCUSSION

This study provides evidence for the release of vesicular Zn^{2+} by showing Zn^{2+} exocytosis directly from presynaptic mossy fiber boutons. Membrane depolarization by high-concentration extracellular potassium and electrical stimulation induces significant Zn^{2+} depletion in the mossy fiber boutons, indicating the release of vesicular Zn^{2+} at the MF→CA3 circuit. This release of vesicular Zn^{2+} is sensitive to Zn^{2+}-specific chelators and is dependent on the influx of extracellular Ca^{2+} in a manner similar to commonly described neurotransmitters. Blocking vesicular reloading of spontaneously released Zn^{2+} by specifically inhibiting the vacuolar-type H^+-ATPase depletes (reduces) vesicular Zn^{2+} in the mossy fiber boutons. Our data demonstrate that some mechanism exists for the uptake of synaptically released Zn^{2+} during transmission. Finally, the present study directly demonstrates the translocation of synaptically released Zn^{2+} into postsynaptic neurons, a feature unique to this divalent metal ion, suggesting that Zn^{2+} may function as a transsynaptic anterograde messenger in the hippocampus.

Overwhelming data suggest that histochemically active Zn^{2+} is compartmentalized and concentrated within the synaptic vesicles of the presynaptic boutons of the MF→CA3 circuit (for review see Frederickson et al., 2000). In agreement with these findings, our data support the viewpoint that histochemically active Zn^{2+} is concentrated within the synaptic vesicles of the mossy fiber boutons with images that clearly show bright intracellular Zn^{2+} fluorescence in the presynaptic stratum lucidum (not the stratum pyramidale) of the CA3 hippo-

campal region (Fig. 1B–D) matching Timm's stain (Fig. 1A). The sensitivity of our recorded signals to Zn^{2+}-specific chelators further supports the conclusion that we are observing changes resulting from the binding of histochemically active, labile Zn^{2+}. Essentially, our experimental model allows distinct and simultaneous examination of both pre- and postsynaptic events of Zn^{2+} fluctuation during neural activity, representing the first time such a technique has been described. Many models of synaptic transmission have been developed at the postsynaptic level, but few techniques exploring presynaptic events have been demonstrated. This likely is due to the diminutive size of the nerve terminals in the brain as well as the nature of electrophysiological and imaging techniques, many of which involve manipulations of postsynaptic membrane currents, membrane potentials, or cellular signaling pathways to create some observable effect. In our experiments, there was a clear distinction between morphological layers of the hippocampus loaded with Zinpyr-1 (Fig. 1A–E), allowing comparisons between presynaptic and postsynaptic fluctuations in Zn^{2+} concentrations, which should be useful to researchers employing slices from whole brains rather than cultured neurons. We believe that the dynamic visualization of intracellular Zn^{2+} described in this study combined with other fluorescent probes and tracers will be an asset to future investigations of the complex processes of cellular trafficking and signaling involved in Zn^{2+} homeostasis.

By measuring the Zn^{2+} concentrations in the extracellular space or perfusate, previous research has suggested that vesicular Zn^{2+} in the mossy fiber boutons undergoes release in a manner similar to commonly
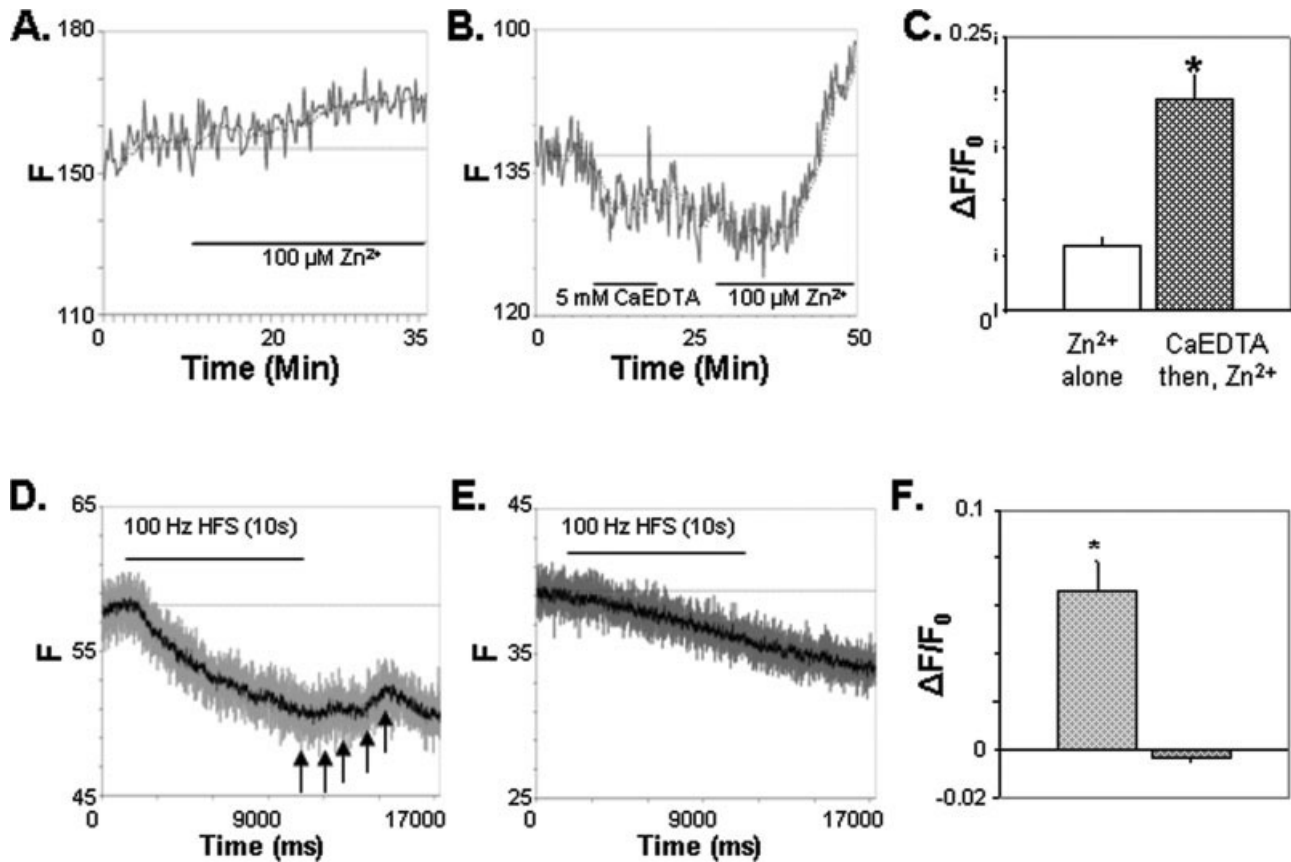
Fig. 6. Properties of presynaptic Zn^{2+} uptake. **A:** Treatment with 100 μM Zn^{2+} yielded a fluorescent increase recorded from the presynaptic region of the MF→CA3 synapse. **B:** Treatment with 5 mM exogenous CaEDTA caused a reduction in presynaptic fluorescence, indicating the deduction of vesicular Zn^{2+} from the presynaptic mossy fiber terminals by the chelator. Subsequent treatment with 100 μM exogenous Zn^{2+} showed fluorescence increases in the presynaptic mossy fiber area, indicating that prechelation of vesicular Zn^{2+} reduces necessary Zn^{2+} storages (in vesicles) and enhances exogenous Zn^{2+} uptake. **C:** Bar graph summarizing the data of fluorescence change data. Fluorescence for the 5-mM-CaEDTA group showed a significantly greater increase than the Zn^{2+}-only group (Zn^{2+}-only group mean = 0.0579 ± 0.01, 5-mM-CaEDTA group mean = 0.19 ± 0.02, n = 7, ★$P < 0.001$). **D:** By using confocal line scans in the stratum lucidum of the CA3 region of the hippocampus, a high temporal resolution could be obtained. Treatment of Zinpyr-1-loaded slices with high-frequency electrical stimula-tion (100 Hz, 0.3 mA, 10 sec) resulted in a decrease in fluorescence from line scans in the stratum lucidum of CA3, indicating the release of vesicular Zn^{2+} from the mossy fiber terminals in response to depolarizing stimulus. Immediately following the stimulus, a resurging fluorescent transient (arrows) was observed, indicating the reuptake of synaptically released Zn^{2+}. **E:** By applying high-frequency electrical stimulation in the presence of 5 mM CaEDTA, the fluorescence hump was eliminated, indicating that the chelator dynamically bound Zn^{2+} released from the mossy fiber terminals and prevented Zn^{2+} reuptake to presynaptic boutons. **F:** Bar figure of ΔF/F₀ values for the above-described experiments. (F_0 was determined by averaging the last 100 fluorescence readings prior to termination of high-frequency stimulation.) The resurging fluorescence transient (hump) in untreated slices was significantly greater than that observed in slices treated with HFS in the presence of CaEDTA [untreated mean = 0.066 ± 0.013 (green bar), CaEDTA-treated mean = −0.0032 ± 0.0019 (red bar), n = 7, ★$P < 0.001$].

described neurotransmitters, being both Ca^{2+} dependent and tetrodotoxin sensitive (Li et al., 2001b; Ueno et al., 2002; Qian and Noebels, 2005). In these reports, increases in $[Zn^{2+}]_o$ have been shown to be achievable via the application of physiologically relevant stimuli, being induced by both electrical stimulation and depolarization of the neuronal membrane by increasing concentrations of extracellular K^+. However, in part because of the method of measuring elevated Zn^{2+} levels indirectly in the extracellular space, the source of Zn^{2+} accumulation in these studies has been a matter of

debate (Bastian and Li, 2007). Results in the present study support the release of Zn^{2+} by directly demonstrating vesicular Zn^{2+} exocytosis from mossy fiber boutons (Figs. 2, 4). Zn^{2+} exocytosis is further shown to be calcium dependent, being arrested by calcium channel blockade and by perfusion of Ca^{2+}-free media (Fig. 3).

Our experiments with concanamycin A (Fig. 5) provide evidence for a mechanism of Zn^{2+} loading into synaptic vesicles that is dependent on the proton electrochemical gradient generated by the vacuolar H^+-ATPase

in a manner similar to glutamate (see also Cavelier and Attwell, 2007). It is likely that glutamate and Zn^{2+} are actively sequestered and stored within the same vesicles (Perez-Clausell and Danscher, 1985; Beaulieu et al., 1992; Wenzel et al., 1997), but it may be that they are stored in wholly separate vesicles and merely undergo simultaneous release. Future studies are needed to clarify this issue. Furthermore, the data also indicate that blocking vesicular loading by inhibition of the vacuolar-type H^+-ATPase is sufficient to deplete readily releasable Zn^{2+} over time. Taken together, these data indicate that Zn^{2+} undergoes vesicular loading that is dependent on the proton electrochemical gradient in a manner similar to other neurotransmitters. The implications of the kinetics of Zn^{2+} release with respect to neuronal activation and the physiological function of Zn^{2+} will have to be clarified in future studies.

Despite ample evidence to support the release of Zn^{2+} in a manner similar to common neurotransmitters, scarcely any progress has been made since the original description of the reuptake of synaptically released Zn^{2+} by Frederickson and his colleagues more than 20 years ago (Howell et al., 1984). It now appears that Zn^{2+} is sequestered into synaptic vesicles by the specific Zn^{2+} transporter ZnT3 (Palmiter et al., 1996; Wenzel et al., 1997; Cole et al., 1999). However, the mechanisms involved in the cellular trafficking of Zn^{2+} to boutons are still enigmatic. If Zn^{2+} has a neurotransmitter-like function, then some mechanism must exist to maintain transient Zn^{2+} stores and replenish vesicular contents following neuronal activities. Speculative models of transport include conceptual processes by which Zn^{2+} traverses the distance between the cell body and nerve terminals (Colvin et al., 2003). Here we show that the decrease of vesicular Zn^{2+} by chelation is reversible by subsequently exposing the cells to exogenous Zn^{2+} (Fig. 6), suggesting a mechanism of uptake within the presynaptic terminals. Our data also suggest that synaptically released Zn^{2+} may undergo reuptake to mossy fiber boutons. This reuptake of synaptically released (endogenous) Zn^{2+} is abolished by a Zn^{2+}-specific chelator that dynamically binds and removes Zn^{2+} in the synaptic cleft upon release.

The cytoplasmic levels of Zn^{2+} are probably regulated by zinc influx and efflux transporters. The presence of the high-affinity Zn^{2+}-specific transporter ZnT3 may also help maintain a low concentration of cytoplasmic Zn^{2+} in the mossy fiber boutons by loading free Zn^{2+} into synaptic vesicles. Active sequestration and vesicularization of Zn^{2+} consequently create a concentration gradient across the membrane, with cytosolic concentrations of free Zn^{2+} in the picomolar range (Krezel and Maret, 2006). Previous research has estimated the concentration of synaptically released Zn^{2+} at the cleft to reach as high as 10 μM (Vogt et al., 2000; Li et al., 2001b), implying that the concentration difference between the cytosol of the presynaptic boutons and the extracellular space could be as high as 1,000-fold (pM to μM). Zn^{2+} uptake following neurotransmission could

therefore be like that described for other ions: a passive process in which Zn^{2+} moves from an area of high concentration in the synaptic cleft to an area of low concentration within the presynaptic cytosol, a process we would expect to be mediated by as yet unidentified ion pores or channels.

Our data indicate that Zn^{2+} release, unlike release of conventional neurotransmitters, is coupled with a rise in the cytosolic Zn^{2+} in postsynaptic neurons. The ability of Zn^{2+} to enter postsynaptic cells and directly affect intracellular signaling pathways truly demands a reconsideration of the conventional concept of synaptically released substances as molecules that bind surface receptor proteins and exert their influences by changing the permeability of membrane channels or the activation states of second messengers. It is reasonable to expect the translocation of synaptically released Zn^{2+} under physiological conditions to be through divalent metal cation-permeable, glutamate-activated postsynaptic channels. Coreleased glutamate can promote Zn^{2+} entry into the neuron by opening Zn^{2+}-permeable AMPA/kainate channels directly (e.g., Ca^{2+}-A/K; Yin and Weiss, 1995) or indirectly through depolarization of the membrane (e.g., voltage-dependent calcium channels; Li et al., 2002). Zn^{2+} translocation into postsynaptic neurons would thus not take place unless both presynaptic release and postsynaptic channel opening occurred simultaneously. Previously, we reported translocation by electrical stimulation (at mossy fibers), a method that results in the synaptic release of both Zn^{2+} and glutamate (Li et al., 2001b). The translocation of synaptically released Zn^{2+} raises the intriguing possibility that Zn^{2+} may interact with many cytosolic macromolecules in the postsynaptic cell (Vallee and Falchuk, 1993; Hubbard et al., 1991; Park and Koh, 1999; Lengyel et al., 2000).

What remains largely unclear is the function of the vesicular Zn^{2+}. Recent studies on the physiological actions of synaptically released Zn^{2+} indicate that synaptic Zn^{2+} modulates the functions of NMDA receptors (Vogt et al., 2000) and glycine receptors (Hirzel et al., 2006) and plays a role in synaptic plasticity (Li et al., 2001a; Kodirov et al., 2006). While the search for the function of synaptic Zn^{2+} continues, once a definitive role for this metal transmission ion in neurotransmission has been identified, a reconsideration of the classic definition of neurotransmitters will be unavoidable. Zinc may very well be an example of a new class of neurotransmitter in the form of divalent metal cations. If the ions involved in synaptic transmission can themselves function as neurotransmitters, clearly the classic picture of transmission must be expanded to include explanations for the events that we and others have now documented.

thanks his graduate advisory committee Drs. Robert Colvin, William Holmes, and Daewoo Lee for critical comments on experimental data.

REFERENCES

Aniksztejn L, Charton G, Ben-Ari Y. 1987. Selective release of endogenous zinc from the hippocampal mossy fibers in situ. Brain Res 404:58–64.

Assaf SY, Chung SH. 1984. Release of endogenous Zn^{2+} from brain tissue during activity. Nature 308:734–736.

Bastian C, Li YV. 2007. Fluorescence imaging study of extracellular zinc at the hippocampal mossy fiber synapse. Neurosci Lett 419:119–124.

Beaulieu C, Dyck R, Cynader M. 1992. Enrichment of glutamate in zinc-containing terminals of the cat visual cortex. Neuroreport 3:861–864.

Bowman EJ, Siebers A, Altendorf K. 1988. Bafilomycins: a class of inhibitors of membrane ATPases from microorganisms, animal cells, and plant cells. Proc Natl Acad Sci U S A 85:7972–7976.

Buhl EH, Otis TS, Mody I. 1996. Zinc-induced collapse of augmented inhibition by GABA in a temporal lobe epilepsy model. Science 271:369–373.

Burdette SC, Walkup GK, Spingler B, Tsien RY, Lippard SJ. 2001. Fluorescent sensors for Zn^{2+} based on a fluorescein platform: synthesis, properties and intracellular distribution. J Am Chem Soc 123:7831–7841.

Cavelier P, Attwell D. 2007. Neurotransmitter depletion by bafilomycin is promoted by vesicle turnover. Neurosci Lett 412:95–100.

Cole TB, Wenzel HJ, Kafer KE, Schwartzkroin PA, Palmiter RD. 1999. Elimination of zinc from synaptic vesicles in the intact mouse brain by disruption of the ZnT3 gene. Proc Natl Acad Sci U S A 96:1716–1721.

Colvin RA, Fontaine CP, Laskowski M, Thomas D. 2003. Zn^{2+} transporters and Zn^{2+} homeostasis in neurons. Eur J Pharmacol 479:171–185.

Danscher G. 1981. Histochemical demonstration of heavy metals. A revised version of the sulphide silver method suitable for both light and electronmicroscopy. Histochemistry 71:1–16.

Davis JP, Tikunova SB, Walsh MP, Johnson JD. 1999. Characterizing the response of calcium signal transducers to generated calcium transients. Biochemistry 38:4235–4244.

Fisher JL, Macdonald RL. 1998. The role of an alpha subtype M2-M3 His in regulating inhibition of GABAA receptor current by zinc and other divalent cations. J Neurosci 18:2944–2953.

Frederickson CJ, Bush AI. 2001. Synaptically released zinc: physiological functions and pathological effects. Biometals 14:353–366.

Frederickson CJ, Suh SW, Silva D, Thompson RB. 2000. Importance of zinc in the central nervous system: the zinc-containing neuron. J Nutr 130:1471S–1483S.

Frederickson CJ, Suh SW, Koh JY, Cha YK, Thompson RB, LaBuda CJ, Balaji RV, Cuajungco MP. 2002. Depletion of intracellular zinc from neurons by use of an extracellular chelator in vivo and in vitro. J Histochem Cytochem 50:1659–1662.

Frederickson CJ, Koh JY, Bush AI. 2005. The neurobiology of zinc in health and disease. Nat Rev Neurosci 6:449–462.

Goldsmith CR, Lippard SJ. 2006. Analogues of zinpyr-1 provide insight into the mechanism of zinc sensing. Inorg Chem 45:6474–6478.

Haug FM. 1967. Electron microscopical localization of the zinc in hippocampal mossy fiber synapses by a modified sulfide silver procedure. Histochemie 8:355–368.

Hirzel K, Muller U, Latal AT, Hulsmann S, Grudzinska J, Seeliger MW, Betz H, Laube B. 2006. Hyperekplexia phenotype of glycine receptor alpha1 subunit mutant mice identifies Zn^{2+} as an essential endogenous modulator of glycinergic neurotransmission. Neuron 52:679–690.

Howell GA, Welch MG, Frederickson CJ. 1984. Stimulation-induced uptake and release of zinc in hippocampal slices. Nature 308:736–738.

Hubbard SR, Bishop WR, Kirschmeier P, George SJ, Cramer SP, Hendrickson WA. 1991. Identification and characterization of zinc binding sites in protein kinase C. Science 254:1776–1779.

Huss M, Ingenhorst G, Konig S, Gassel M, Drose S, Zeeck A, Altendorf K, Wieczorek H. 2002. Concanamycin A, the specific inhibitor of V-ATPases, binds to the V(o) subunit c. J Biol Chem 277:40544–40548.

Kodirov SA, Takizawa S, Joseph J, Kandel ER, Shumyatsky GP, Bolshakov VY. 2006. Synaptically released zinc gates long-term potentiation in fear conditioning pathways. Proc Natl Acad Sci U S A 103:15218–15223.

Krezel A, Maret W. 2006. Zinc-buffering capacity of a eukaryotic cell at physiological pZn. J Biol Inorg Chem 11:1049–1062.

Lengyel I, Fieuw-Makaroff S, Hall AL, Sim AT, Rostas JA, Dunkley PR. 2000. Modulation of the phosphorylation and activity of calcium/calmodulin-dependent protein kinase II by zinc. J Neurochem 75:594–605.

Li Y, Hough CJ, Frederickson CJ, Sarvey JM. 2001a. Induction of mossy fiber→Ca3 long-term potentiation requires translocation of synaptically released Zn^{2+}. J Neurosci 21:8015–8025.

Li Y, Hough CJ, Suh SW, Sarvey JM, Frederickson CJ. 2001b. Rapid translocation of Zn^{2+} from presynaptic terminals into postsynaptic hippocampal neurons after physiological stimulation. J Neurophysiol 86:2597–2604.

Li Y, Hough CJ, Suh SW, Frederickson CJ, Sarvey JM. 2002. Translocation of synaptically released zinc involves voltage dependent calcium channels (vdccs) in rat hippocampal ca3 pyramidal neurons. Program No. 437:12. 2002 Abstract Viewer/Neuroscience Meeting Planner. Washington, DC: Society for Neuroscience.

Martell AE, Smith RM. 1974. Critical stability constants, vol. 1. Plenum Press, New York.

Mothet JP, Pollegioni L, Ouanounou G, Martineau M, Fossier P, Baux G. 2005. Glutamate receptor activation triggers a calcium-dependent and SNARE protein-dependent release of the gliotransmitter D-serine. Proc Natl Acad Sci U S A 102:5606–5611.

Palmiter RD, Cole TB, Quaife CJ, Findley SD. 1996. ZnT-3, a putative transporter of zinc into synaptic vesicles. Proc Natl Acad Sci U S A 93:14934–14939.

Park JA, Koh JY. 1999. Induction of an immediate early gene egr-1 by zinc through extracellular signal-regulated kinase activation in cortical culture: its role in zinc-induced neuronal death. J Neurochem 73:450–456.

Perez-Clausell J, Danscher G. 1985. Intravesicular localization of zinc in rat telencephalic boutons. A histochemical study. Brain Res 337:91–98.

Perez-Clausell J, Danscher G. 1986. Release of zinc sulphide accumulations into synaptic clefts after in vivo injection of sodium sulphide. Brain Res 362:358–361.

Peters S, Koh J, Choi DW. 1987. Zinc selectively blocks the action of N-methyl-D-aspartate on cortical neurons. Science 236:589–593.

Qian J, Noebels JL. 2005. Visualization of transmitter release with zinc fluorescence detection at the mouse hippocampal mossy fiber synapse. J Physiol 566:747–758.

Rassendren FA, Lory P, Pin JP, Nargeot J. 1990. Zinc has opposite effects on NMDA and non-NMDA receptors expressed in Xenopus oocytes. Neuron 4:733–740.

Smart TG, Xie X, Krishek BJ. 1994. Modulation of inhibitory and excitatory amino acid receptor ion channels by zinc. Prog Neurobiol 42:393–341.

Ueno S, Tsukamoto M, Hirano T, Kikuchi K, Yamada MK, Nishiyama N, Nagano T, Matsuki N, Ikegaya Y. 2002. Mossy fiber Zn^{2+} spillover modulates heterosynaptic N-methyl-D-aspartate receptor activity in hippocampal CA3 circuits. J Cell Biol 158:215–220.

Vallee BL, Falchuk KH. 1993. The biochemical basis of zinc physiology. Physiol Rev 73:79–118.

Vogt K, Mellor J, Tong G, Nicoll R. 2000. The actions of synaptically released zinc at hippocampal mossy fiber synapses. Neuron 26:187–196.

Wenzel HJ, Cole TB, Born DE, Schwartzkroin PA, Palmiter RD. 1997. Ultrastructural localization of zinc transporter-3 (ZnT-3) to synaptic vesicle membranes within mossy fiber boutons in the hippocampus of mouse and monkey. Proc Natl Acad Sci U S A 94:12676–12681.

Westbrook GL, Mayer ML. 1987. Micromolar concentrations of Zn^{2+} antagonize NMDA and GABA responses of hippocampal neurons. Nature 328:640–643.

Woodroofe CC, Masalha R, Barnes KR, Frederickson CJ, Lippard SJ. 2004. Membrane-permeable and -impermeable sensors of the Zinpyr family and their application to imaging of hippocampal zinc in vivo. Chem Biol 11:1659–1666.

Yin HZ, Weiss JH. 1995. Zn^{2+} permeates Ca^{2+} permeable AMPA/kainate channels and triggers selective neural injury. Neuroreport 6:2553–2556.